AGN selection by 18-band SED fitting in mid-infrared in the *AKARI* NEP deep field

Ting-Chi Huang,[1] Tomotsugu Goto,[1] Tetsuya Hashimoto,[1] Nagisa Oi,[2] and Hideo Matsuhara[3]

[1]*Institute of Astronomy, National Tsing Hua University, No. 101, Section 2, Kuang-Fu Road, Hsinchu, Taiwan 30013*

[2]*Tokyo University of Science, 1-3 Kagurazaka, Shinjuku-ku, Tokyo 162-8601, Japan*

[3]*Institute of Space and Astronautical Science, Japan Aerospace Exploration Agency, 3-1-1 Yoshinodai, Chuo, Sagamihara, Kanagawa 252-5210, Japan*

ABSTRACT

In this research, we provide a new, efficient method to select infrared (IR) active galatic nucleus (AGN). In the past, AGN selection in IR had been established by many studies using color-color diagrams, because the number of filters of IR telescopes is limited. The *AKARI* North Ecliptic Pole (NEP) survey was carried out by the *AKARI* Infrared Camera (IRC), which has 9 filters in mid-IR with a continuous wavelength coverage from 2 to 24 μm. Taking advantage of the intrinsically different mid-IR features of AGN and star-forming galaxies (SFGs), we performed SED fitting to separate these two populations by the best-fitting model. In the X-ray AGN sample, our method by SED fitting selects 50% AGNs, while the previous method by colour criteria recovers only 30% of them, which is a significant improvement. Furthermore, in the whole NEP deep sample, SED fitting selects two times more AGNs than the color selection. This may imply that the black hole accretion history could be more stronger than previous estimates.

1. INTRODUCTION

Active Galactic Nucleus (AGN) plays an important role in galaxy evolution. It has been widely known that AGN's powerful energy comes from the accretion of its supermassive black hole (SMBH) and such strong energy can affect the star-forming activity in the host galaxies. Therefore, we can probe how galaxies and SMBHs have evolved with cosmic time by investigating AGNs. As a result, it is fundamental to have an efficient way to select AGNs. However, the X-ray and ultraviolet (UV) light emitted from the accretion disk are tend to be obscured by the dust and gas of AGN torus (e.g., Alexander et al. 2001; Richards et al. 2003; Webster et al. 1995). Under this situation, we fortunately can still detect AGN in IR from the thermal emission from dust. But here comes another problem that not only AGNs, but also star-forming galaxies (SFGs) can be observed in IR due to the polycyclic aromatic hydrocarbon (PAH) emission features at 3.3, 6.2, 7.7, 8.6 and 11.3 μm. Hence, to select AGNs in IR, the separation between AGNs and SFGs is extremely essential and important.

Since AGN has a power-law like spectrum from the dust emission in mid-IR, previous studies frequently used some criteria in color-color diagrams to select AGNs (e.g., Jarrett et al. 2011; Lacy et al. 2004; Richards et al. 2006; Stern et al. 2005). However, selections by colors have a limitation of the number of bands. Futhermore, the observatories used in previous work generally have a detection gap in their wavelength range. For example, *Spitzer* IRAC has 4 filters at 3.6, 4.5, 5.8 and 8.0 μm, but the next closest filter is the MIPS24 at 24 μm. *AKARI* Infrared Camera (IRC) is equipped with 9 filters in mid-IR, which continuously covers the wavelength range from 2 to 24 μm (Matsuhara et al. 2006). The *AKARI* IRC 9 bands in mid-IR allow us to separate AGNs and SFGs by SED fitting. In this work, we combined the mid-IR photometry from *AKARI*, *WISE* and *Spitzer* and performed SED fitting with 25 empirical templates to select AGNs by 18 mid-IR bands.

2. DATA AND ANALYSIS

We used the catalogue from the *AKARI* North Ecliptic Pole (NEP) deep survey (Murata et al. 2013) and required that all the objects must be detected in the *AKARI* 18 μm band. In total, we have 5761 objects. In addition to *AKARI*, we also included the data from *GALEX*, CFHT, *WISE*, *Spitzer*, and *Herschel* for SED fitting, but only a part of objects have been detected by each instruments other than *AKARI*. The redshift information of every NEP deep objects were calculated in Oi et al. (2014).

We performed SED fitting by LEPHARE code to select AGNs. In the SED fitting, the UV and optical data are used to fit with stellar components (Coleman et al. 1980; Kinney et al. 1996), and the mid-IR data are used to fit with the models of AGNs and SFGs (Polletta et al. 2007). After the fitting, the following criteria (Huang et al. 2017) were requested to

eliminate badly-fit results in our sample. "(1) An object must have a best-fitting model. (2) The object must have a redshift value. (3) The number of bands used in the IR fitting must be equal to or larger than 3." We have 4833 objects in the final sample and we name it "the SED sample." To separate stars and galaxies, we followed the suggestion in Oi et al. (2014) using the CLASS_STAR parameter from the CFHT source extraction software, SExtractor, of the CFHT z'-band.

3. RESULTS

3.1. AGN selection

We selected AGN in the galaxy sample by checking the best-fitting model. We used the SWIRE templates (Polletta et al. 2007) to select AGN. The SWIRE templates contain 25 models, and 9 of them are AGN models, which include models of Seyfert 1.8, Seyfert 2, QSO2, QSO1, BQSO1, TQSO1, Mrk231, IRAS19254 and Torus. The other 16 SFGs models contain 3 elliptical galaxies, 7 spiral galaxies and 6 starbursts. Figure 1 shows the summary of AGN selection results from SED fitting and the *WISE* color-color diagram (Wright et al. 2010; Jarrett et al. 2011). In the subsample that all the objects have *WISE* 4-band magnitudes, our SED fitting selects nearly 2 times more AGNs than the criteria in color-color diagram. This result impies that AGN luminosity function and the cosmic black hole accretion history may be much stronger than people expected in the past.
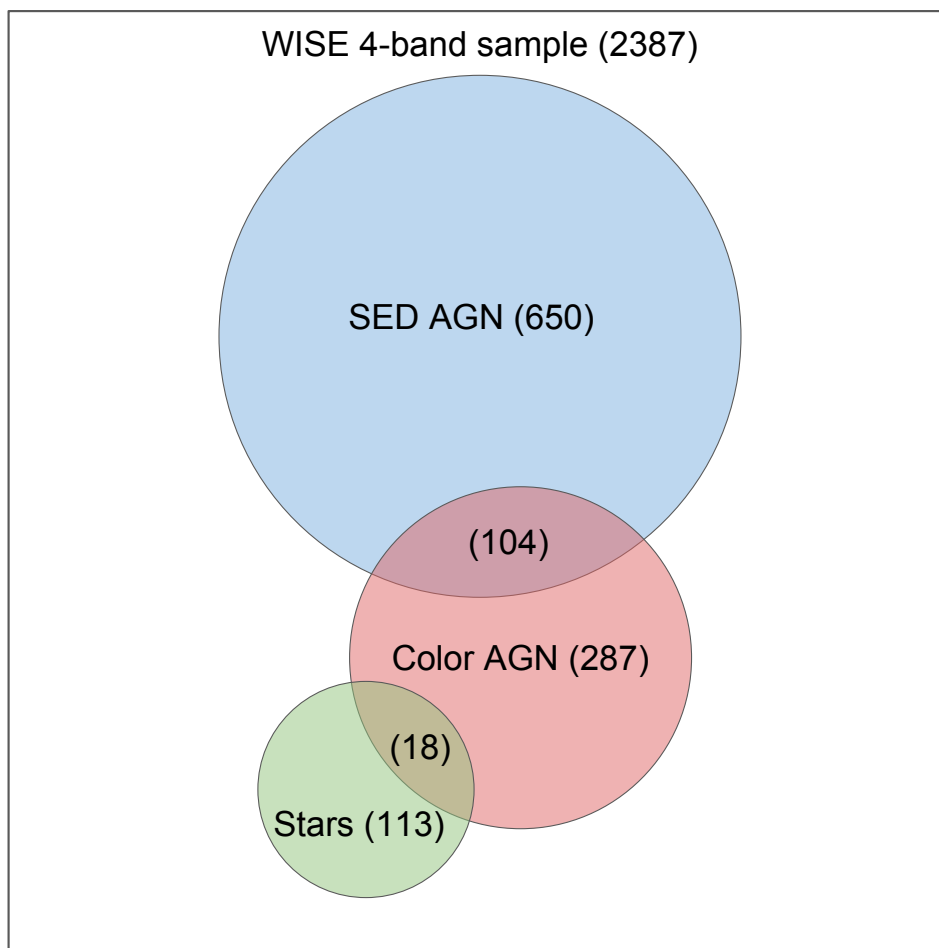

Figure 1. The Venn diagram which shows the AGN selection by our SED fitting and the *WISE* color-color diagram. The numbers in parentheses are the counts of the objects.

3.2. AGNs missed by color selection

There are many AGNs selected by the SED fitting but not by the color criteria. We show those SED AGNs in the *WISE* color-color diagram in Figure 2. The color box is defined to select QSOs, so not surprisingly, there are many Seyfert 1.8 and Seyfert 2 AGN outside of the box. AGNs of these two models are moderately luminous or host-dominated AGNs. Therefore, the result suggests that the *WISE* color box possibly misses some AGNs.
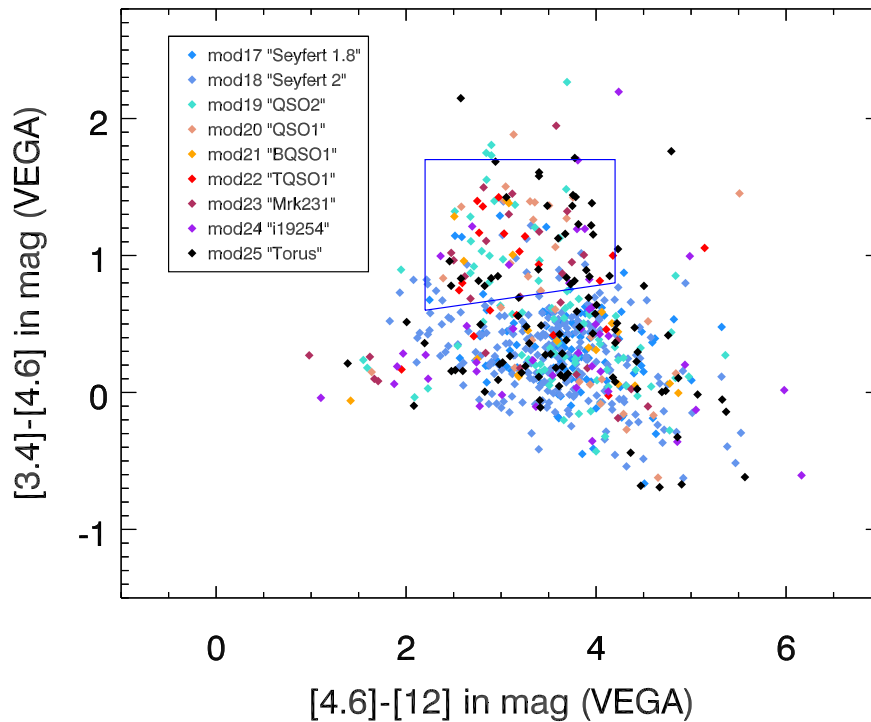
Figure 2. The *WISE* color-color diagram with AGNs selected by our SED fitting. Different models are plotted in different colors as shown in the legend.

3.3. **Examination by X-ray AGN**

The X-ray catalogue of the *AKARI* NEP deep field from Chandra observation (Krumpe et al. 2015) was included to compare the AGN selection by our SED fitting and the *WISE* color-color diagram. We matched the celestial coordinate to combine the X-ray catalogue with the NEP deep catalogue having *WISE* 4-band data in 1 arcsec tolerance radius. There are 254 X-ray objects in total and we regard all the X-ray sources as AGNs in this examination. In this X-ray sample, we compare the number fration of AGNs selected from the *WISE* color-color diagram and our SED fitting. The result shows that our SED fitting recovers more AGNs in the X-ray AGN sample (Figure 3). Moreover, if the number of band used in the SED fitting is larger, the recovering rate will become higher. Also, SED fitting can produce better results in low-redshift sample.

REFERENCES

Alexander, D. M., Brandt, W. N., Hornschemeier, A. E., et al. 2001, AJ, 122, 2156
Coleman, G. D., Wu, C.-C., & Weedman, D. W. 1980, ApJS, 43, 393
Huang, T.-C., Goto, T., Hashimoto, T., Oi, N., & Matsuhara, H. 2017, MNRAS, 471, 4239
Jarrett, T. H., Cohen, M., Masci, F., et al. 2011, ApJ, 735, 112
Kinney, A. L., Calzetti, D., Bohlin, R. C., et al. 1996, ApJ, 467, 38
Krumpe, M., Miyaji, T., Brunner, H., et al. 2015, MNRAS, 446, 911
Lacy, M., Storrie-Lombardi, L. J., Sajina, A., et al. 2004, ApJS, 154, 166
Matsuhara, H., Wada, T., Matsuura, S., et al. 2006, PASJ, 58, 673
Murata, K., Matsuhara, H., Wada, T., et al. 2013, A&A, 559, A132
Oi, N., Matsuhara, H., Murata, K., et al. 2014, A&A, 566, A60
Polletta, M., Tajer, M., Maraschi, L., et al. 2007, ApJ, 663, 81
Richards, G. T., Hall, P. B., Vanden Berk, D. E., et al. 2003, AJ, 126, 1131
Richards, G. T., Lacy, M., Storrie-Lombardi, L. J., et al. 2006, ApJS, 166, 470
Stern, D., Eisenhardt, P., Gorjian, V., et al. 2005, ApJ, 631, 163
Webster, R. L., Francis, P. J., Petersont, B. A., Drinkwater, M. J., & Masci, F. J. 1995, Nature, 375, 469
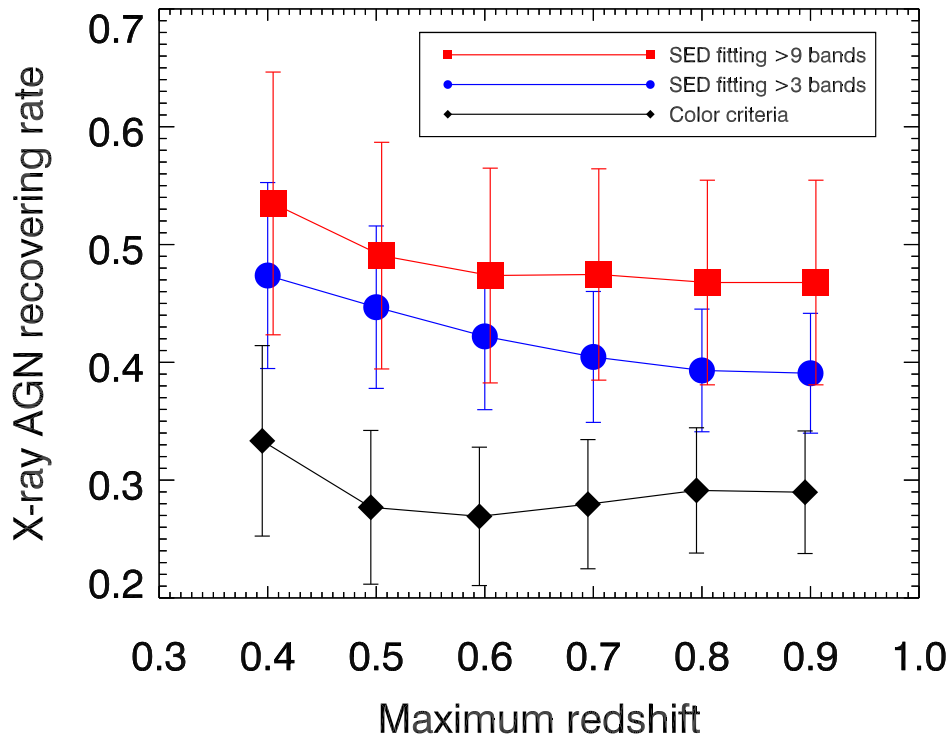Wright, E. L., Eisenhardt, P. R. M., Mainzer, A. K., et al. 2010, AJ, 140, 1868

Figure 3. The X-ray AGN recovering rate of the selection by our SED fitting and the color criteria. The red and blue lines are the results of SED fitting with different number of bands limitations. The black line shows the results from the selection by the *WISE* color-color diagram.